Free disturbances and spot formation: (i) on a surface roughness, (ii) in a near-wake, (iii) under an adverse pressure gradient

F. T. Smith

Department of Mathematics, University College London, Gower Street, London WC1E 6BT

A review is given of recent and continuing theory on initial-value problems arising in a surface-mounted roughness flow, in the near-wake behind a streamlined body or in a boundary layer under an adverse pressure gradient. These concern instability and transition with entire spectra of modes present. In every case the unsteady disturbances evolve through a transient stage before forming spots. Absolute instability can occur. Nonlinear responses in the near-wake case drive the transition point extremely close to the body trailing edge; while in the adverse-gradient case they first affect significantly the spot leading edge and the calmed region behind the spot.

1. Introduction

The present article considers instability and transition in three fluid-flow configurations which are the subjects of recent and continuing research. These are (i) flow over a surface roughness, (ii) the near-wake of a streamlined body, (iii) a boundary layer under an adverse pressure gradient.

Area (i) is addressed by the Savin *et al.*[1] theory. There have been numerous experimental studies on flow transition over an isolated small roughness mounted on a solid surface, or over distributed roughnesses. The experiments cover a wide range of incident flows. A substantial point made clear by many of the experiments is that the initial small disturbances which may lead on to full transition downstream in practice are free disturbances (and intermittent), as distinct from the fixed-frequency type used in traditional boundary-layer stability analyses. This tends to accentuate the theoretical need for studying initial-value problems. There has been little apparent progress so far in direct computational studies, or theoretical works, with regard to major nonlinear three-dimensional developments for free disturbances in roughness-induced transition. The focus of the Savin *et al.* study is therefore on the onset of nonlinear effects in such an initial-value setting, to capture the underlying early physics of the transition(s). Onset, which is related to marginal flow stability, refers to the first occurrence of those nonlinear effects, typically near the top of the roughness element (or possibly upstream) where an inviscid inflectional instability region starts as in Figure 1 *a*. The onset is associated with reduced wave numbers (other wave numbers being stable), a key feature which is coupled with nonlinear theory by Savin *et al.* This takes account of the need to abandon the fixed-frequency or fixed-wavelength restriction, and even the wave concept altogether, in order to tackle roughness-induced flow transition with free disturbances acting. The nonlinear aspect stems from transition theory on three-dimensional unsteady flow properties developing in the form of vortex–wave interactions, from an inflection point in the streamwise velocity profile of the incident boundary layer or sublayer.

Area (ii) concerns disturbance growth in the thin wake behind a stream-lined body[2]. Numerous theoretical investigations of classical type have been made for temporal or spatial instability in wakes. The interest in this study, however, concerns the linear and subsequent nonlinear disturbance development from a general initial value, especially in the near-wake, given that the rest of the wake may be dependent on the near-wake properties. A more analytical and rational approach is fruitful, based on genuine wake-velocity profiles starting from a double boundary-layer-like form just after the trailing edge, rather than the typical model profiles often assumed. The near-wake response, with its undeveloped profiles, is worth studying first. For the flow past a streamlined trailing edge the inflection point originates just outside the tiny region of nonparallel motion where the Navier-Stokes equations apply in full, buried inside the triple-deck structure: then it emerges close to the Hakkinen-Rott near-wake layer as in Figure 1 *b* and it travels downstream inside the lower-deck sublayer motion until, at a finite station (as inflection disappears in the local velocity profile), it migrates normally towards the main deck. The inflection point subsequently enters the full wake just outside the Goldstein near-wake layer. For other trailing-edge configurations the inflection point may or may not accompany closely the Hakkinen-Rott near-wake, depending on the

e-mail: frank@math.ucl.ac.uk

It is a pleasure to dedicate this article to Prof. Satish Dhawan on his eightieth birthday.

velocity profiles sweeping off the upper and lower trailing edges. In all stream-lined configurations, most of the near-wake in effect contains a single interface. There all wave number components are agitated, a property which is found to promote upstream convection of nonlinear disturbances.

Area (iii) is on unsteady travelling (spot) disturbances near the onset of an adverse pressure gradient[3]. On turbine blades there are substantial areas of adverse pressure gradient. These are observed to leave enhanced calmed regions trailing behind a travelling spot disturbance, the calmed regions being of practical importance in the production of extensive patches of laminar or relaminarized flow on the blades. The need for deeper physical understanding of spots was highlighted at the 1997 Minnowbrook workshop on transition in turbomachinery[4]. Stress was placed on the unknown roles, during spot evolution, of adverse pressure gradients, of calmed regions, of separations, of high free-stream turbulence, and on the need for more basic theoretical study. Major issues in spot dynamics concern: the determination of the sharp edges and global shape of the typical spots; the underlying reason for the calmed region, with its advantageous relaminarizing effect; pressure-gradient influences; and the breakdown to shorter length scales inside the spot. As in areas (i), (ii), most flows of real interest have large characteristic Reynolds numbers; and all transients and growing amplitude components of the travelling spot flow should be included. A crucial position for the initiation of the spot is near the point of minimum basic pressure, at the onset

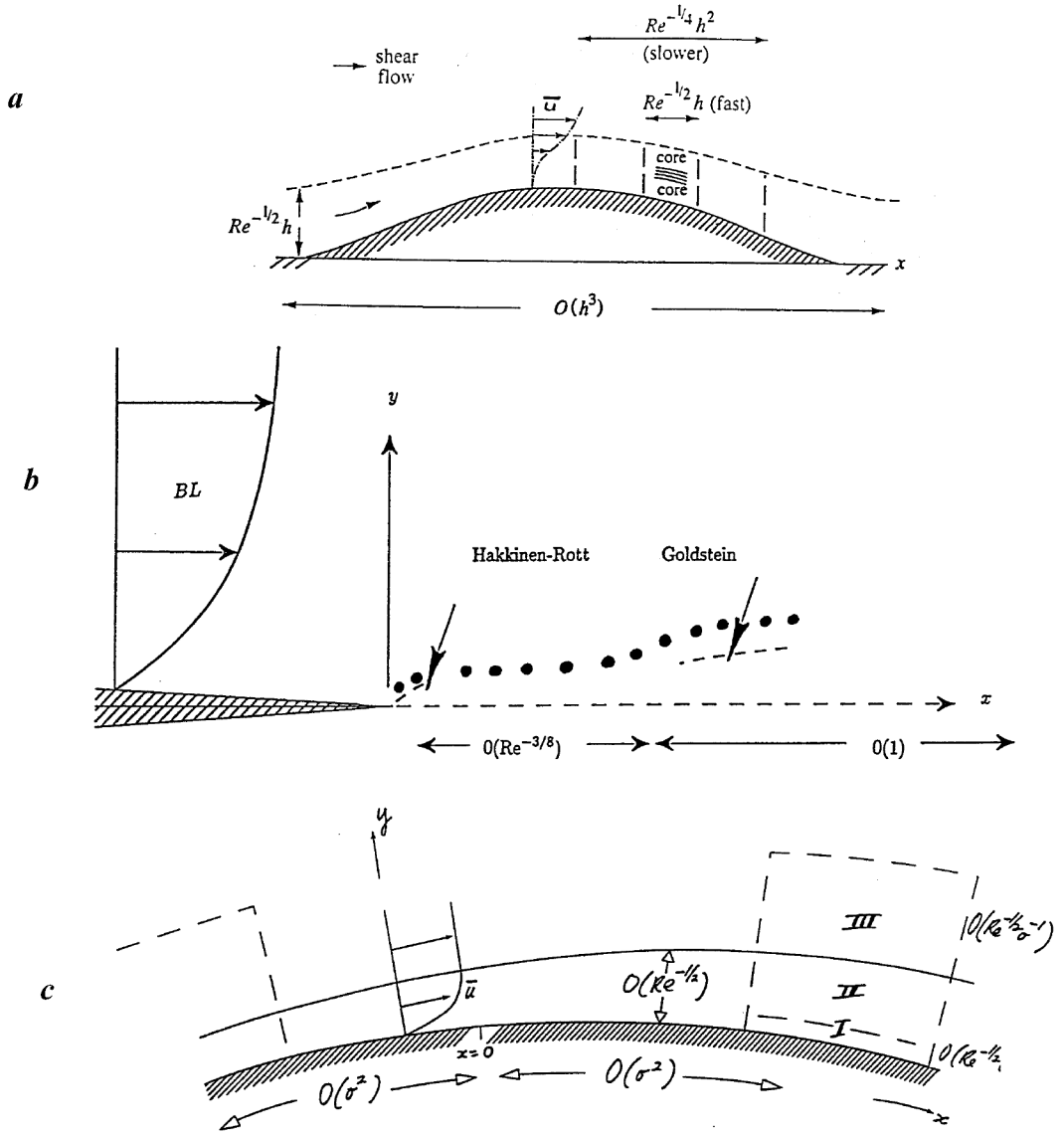

Figure 1. The flow configurations. *a*, Over an isolated roughness (case (i)) for which transition involves core-critical layer interaction in a sublayer. The fraction h is small, so the sublayer is much thinner than the boundary layer; *b*, In a near-wake (case (ii)), as the upper and lower surface boundary layers (BL) sweep past a streamlined trailing edge. Dots show the path of the inflection point; *c*, In a boundary layer at the onset of an adverse pressure gradient (case (iii)). In case (i) the inflection point in the velocity profile $\bar{u}$ is mid-flow but in (iii) it is near the surface. Length scales are indicated.

of the adverse pressure gradient, where inflectional instability enters via a near-wall sublayer as in Figure 1 *c*. Gostelow's experimental spots in particular are initiated there typically, as is the inflectional growth of fixed frequency disturbances in experiments by Dovgal and Kozlov. The present theory is local to that position at first. In the adverse-gradient setting, nonparallel effects need to be incorporated eventually; and, again, although the linear incompressible range should be examined first, the nonlinear range is also to be included in an attempt at providing insight into the calmed region and other mean-flow alterations. The interplay of the pressure gradient with three-dimensionality, nonlinearity and nonparallelism can be considered in turn as in ref. 3.

The common theme is that areas (i)–(iii) involve genuine initial value problems with all modes active, i.e. an entire spectrum, to mirror the practical flow configurations. In each case the free unsteady disturbances pass through an important transient stage initially. Spots then form; the typical Reynolds number Re is large; and each case has a simple result at heart. These simple results are the following, in order:

(i) (*roughness flows*) the integral of $(\bar{u}-c)^{-2}$ across the sublayer must be zero, where $\bar{u}$ is the basic local streamwise velocity profile and the constant c is the inflectional velocity (thus giving frequency proportional to wave number);

(ii) (*near wakes*) the disturbance response to the first approximation is at a constant frequency given by $[\bar{\lambda}]/2$, where $[\bar{\lambda}]$ denotes the jump in velocity slope across the effective interface;

(iii) (*adverse pressure gradients*) the primary response has a frequency proportional to the square of the wave number.

More complicated responses arise at the next order to determine the disturbance amplitude evolution, as described below in §2–4 respectively.

They show the eventual formation of spots, along with various nonlinear effects. In each case due to consideration of space we must draw a veil over most of the background, the solution details, the nondimensionalization, the flow structure and the inherent scales, which are in the original papers. We note, however, that the underlying boundary layer or wake is taken to have conventional normal thickness of order $Re^{-1/2}$ and streamwise scale of order unity. Brief final comments are made in §5.

2. Roughness-induced transition

The roughness element considered is smooth, buried well within the boundary layer and has small streamwise length and a height much less than the boundary-layer thickness. Then physical reasoning suggests concentrating primarily on the height and corresponding sublayer thickness in order-of-magnitude terms at which the basic motion can yield sufficiently strong inflection points for inviscid instability to arise (see Figure 1 *a*). The basic flow past the roughness is then governed by the nonlinear interactive boundary-layer description in the sublayer, with the wall pressure adjusting to satisfy a displacement condition of the form $\bar{u} \sim \bar{y} + \bar{a}$ at the outer edge of the sublayer, where the shear is normalized to unity for convenience. Here $\bar{a}$ is zero for so-called condensed flows. Instability in these basic planar roughness flows with shear was considered in the 1980s, showing that the onset of inflectional instability (with the inflection point typically being in the middle of the sublayer) occurs at an 0(1) finite relative height of the roughness element in general. We then address the three-dimensional inflectional transition.

At leading order a simple long wave solution of the Rayleigh disturbance equation holds, for the $\bar{u}$ given above. Hence as anticipated in the introduction for area (i) the criterion

$$(\mathrm{FP}) \int_0^\infty (\bar{u}-c)^{-2}\,\mathrm{d}\bar{y} = 0, \tag{1}$$

emerges, where FP signifies the finite part. This is followed by the amplitude equation for the general initial input at the next order. No assumption of wave dependence is required. The resulting nonlinear amplitude evolution takes place in a frame moving with velocity c, which is also a real group velocity in essence. The main amplitude equation for the pressure Laplacian $R(X, Z, T)$ in terms of scaled coordinates X, Z (streamwise, spanwise) and time T is

$$\bar{A}_r\left[\frac{\partial R}{\partial T}\right] - \frac{\bar{A}_i}{\pi}\left[\frac{\partial}{\partial T}(PV)\int_{-\infty}^{\infty}\frac{R\,\mathrm{d}\xi}{(X-\xi)}\right]$$

$$= \bar{B}(\bar{x}^*+cT)\frac{\partial R}{\partial X} + \bar{C}\frac{\partial}{\partial X} + \bar{D}\frac{\partial}{\partial X}\int_X^\infty \frac{R\,\mathrm{d}\xi}{(\xi-X)^{1/2}} - \frac{\partial N}{\partial X}, \tag{2}$$

where the constants $\bar{B}, \bar{C}, \bar{D}, \bar{x}^*$ are real, while $\bar{A}$ is usually complex, and

$$\equiv (\mathrm{PV})\int_{-\infty}^{\infty}\int_{-\infty}^{\infty}\frac{\nabla^2 R(\xi,\eta,T)\,\mathrm{d}\xi\,\mathrm{d}\eta}{\{(X-\xi)^2+(Z-\eta)^2\}^{1/2}}. \tag{3}$$

Here PV denotes the principal value. The contribution N is the nonlinear effect which can be of amplitude

squared or cubed form. For linear disturbances eqs (2), (3) yield, at large times, a travelling spot containing exponentially growing amplitude and based on the expanding coordinates $(X, Z) = T(\overline{X}, \overline{Z})$. Examples obtained by Brown and Smith[5] are given in Figure 2, which shows the spot planforms under various conditions. It is interesting that the working extends also to negative c. Some flow conditions, therefore, provoke backward moving spots, implying the presence of absolute and upstream convective instability then.

For nonlinear disturbances, many examples are presented by Savin *et al.*[1], for special types of input. One such is given in Figure 3. Typically complicated short scale behaviour occurs at increased times, with amplitude blow-up or saturation or continued growth being found, depending on the coefficients in the amplitude equation.

3. Near-wake transition

The flow in near wakes has an involved structure. This is such that the basic local steady motion (u, v) there can

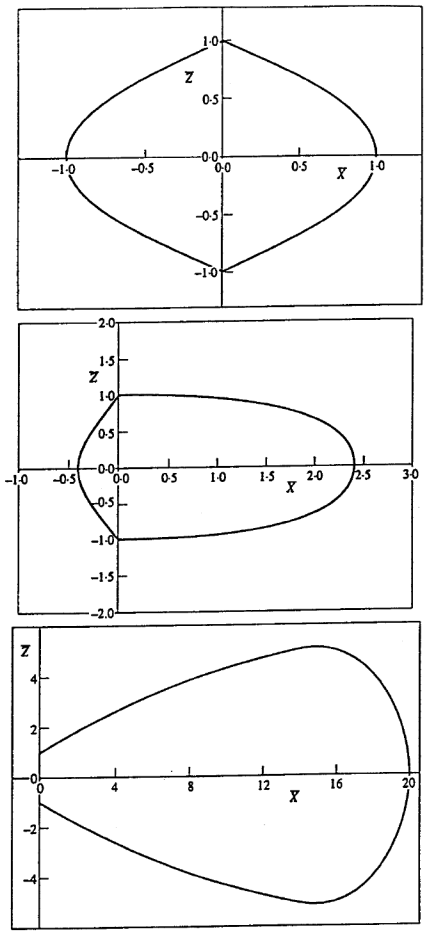

Figure 2. The planforms of spots formed at large times (roughness case) for: top, large adverse parameter G; middle, medium G; bottom, small G.

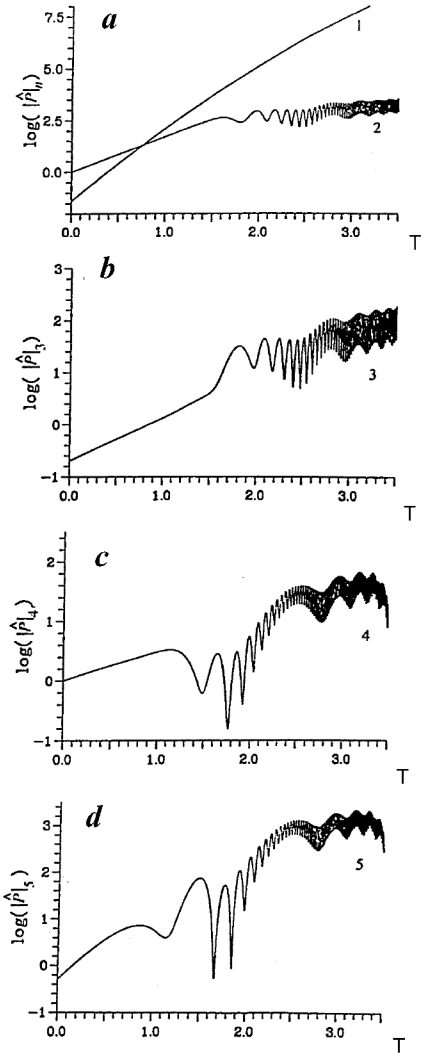

Figure 3. Nonlinear amplitude solution in roughness transition, showing five Fourier components $|\hat{P}_n|$, $n = 1$ to 5, vs time.

be regarded as providing either a quasi-parallel full, nontrivial, wake velocity profile $\overline{u}(y)$, so that

$$(u, v) = (\overline{u}(y), 0) \tag{4}$$

in effect, or nearly uniform shear flow such that

$$(u, v) = (\pm y + \varepsilon \overline{u}_1(y), 0), \tag{5}$$

or

$$(u, v) = (\pm y, \mp \varepsilon B). \tag{6}$$

Again see Figure 1 *b*. Here eqs (4)–(6) all hold to within a multiplicative constant. The parameter ε in cases (5), (6) is small and positive, the distortion $\overline{u}_1(y)$ giving nonzero profile curvature, while the term B is a positive constant due to the viscous Hakkinen-Rott influx velocity (variously described as the suction, entrainment or

mass flux into the Hakkinen-Rott layer), and y 0 respectively.

All three basic flows above are considered by Smith *et al.* but here we highlight (5), (6), especially the latter. The leading-order planar disturbance solution then has simple exponential forms above and below the interface $y = 0$, from which the interface conditions give the non-dimensional dispersion relation

$$\omega = sgn(\alpha), \tag{7}$$

with $\omega(\equiv \alpha c)$ denoting the frequency response for wave number α. So at this level the flow solution reacts at a fixed frequency for any wave number α, corresponding to the dimensional result for area (ii) quoted in the introduction.

At the next level the influences of $\bar{u}_1$, B and nonlinearity are felt. The resulting amplitude (Q_2) equation takes the form

$$4\frac{\partial Q_2}{\partial T} = \frac{2}{\pi}\int_{-\infty}^{\infty}(g_1 + ig_2)Q_2^*(\alpha, T)\exp[i\alpha x]\,d\alpha + 4B\overline{(\ \ _2)} + J_1 - \overline{(J_2)}, \tag{8}$$

with $g_1(\alpha)$, $g_2(\alpha)$ being growth and dispersive terms associated with $\bar{u}_1$. Also $\overline{\ }$ signifies a planar Cauchy-Hilbert integration and J_1, J_2 are the nonlinear effects. The asterisk denotes the Fourier transform and T, x are the local scaled time and streamwise distance respectively. The governing equation reflects, on its right side, an interplay between linear destabilization (for negative $\bar{u}_1''$), linear stabilization from influx (B) and nonlinear modification.

A representative solution is given in Figure 4. Points of note are the following. The linear and nonlinear initial-value problems studied by Smith *et al.* cover a range of quite general input disturbances. Nonuniform vorticity as represented by the distortion profile $\bar{u}_1(y)$ can have a substantial impact on the linear disturbance evolution in the near-wake, as negative (positive) profile curvature is found to be destabilizing (stabilizing), opposite to the response on a fixed surface. The response in the near-wake actually hinges on the function $y\bar{u}_1''$ in symmetric cases, and on an average in non-symmetric ones, for the current setting. By contrast, in *nonlinear* cases the influx B is extremely important close to the trailing edge as the nonlinear cases yield upstream-convecting disturbances. These are present in the figure. Short scale secondary instability is provoked by the nonlinear effects and this has to be countered by the short scale stability produced by the B effect. The balance not only shows that upstream convection can occur generally in the near wake but also forces the transition point closer to the trailing edge as nonlinearity is increased. The cause of the secondary instability above is the slight streamwise velocity jump induced by higher order nonlinear effects acting at the interface, leading to slight Kelvin-Helmholtz growth, whereas the slight normal velocity jump associated with the value of B (which grows as the trailing edge upstream is approached) always induces secondary stability.

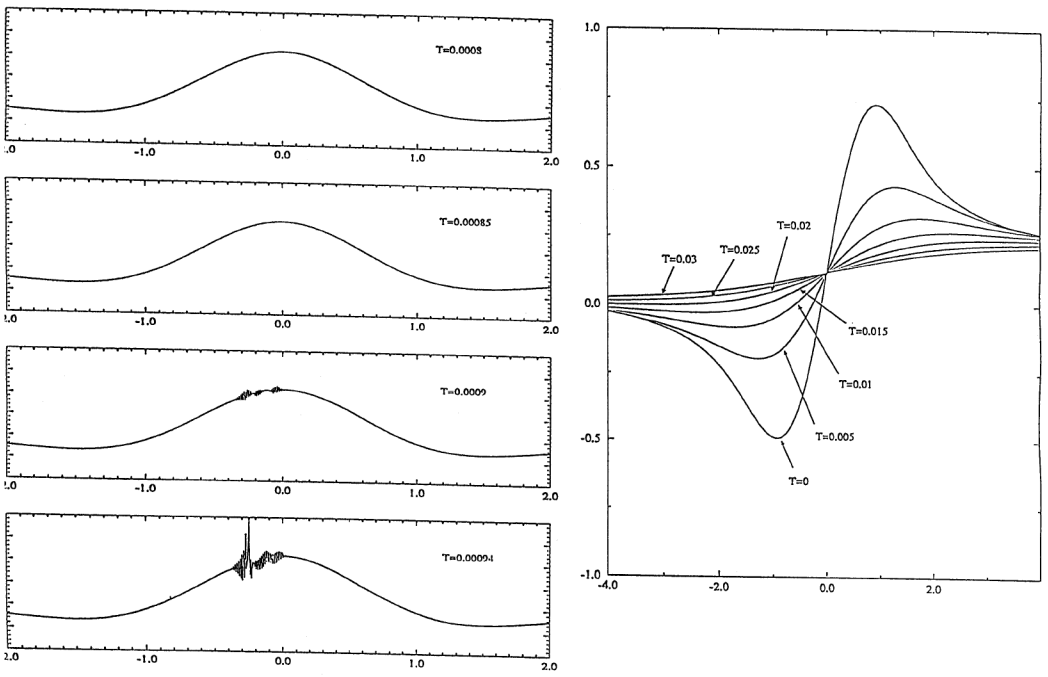

Figure 4. Nonlinear responses (near-wake case), giving temporal development of $\partial Q_2/\partial x$ vs x for zero B on the left and, on the right, Q_2 vs x for $B = 125$.

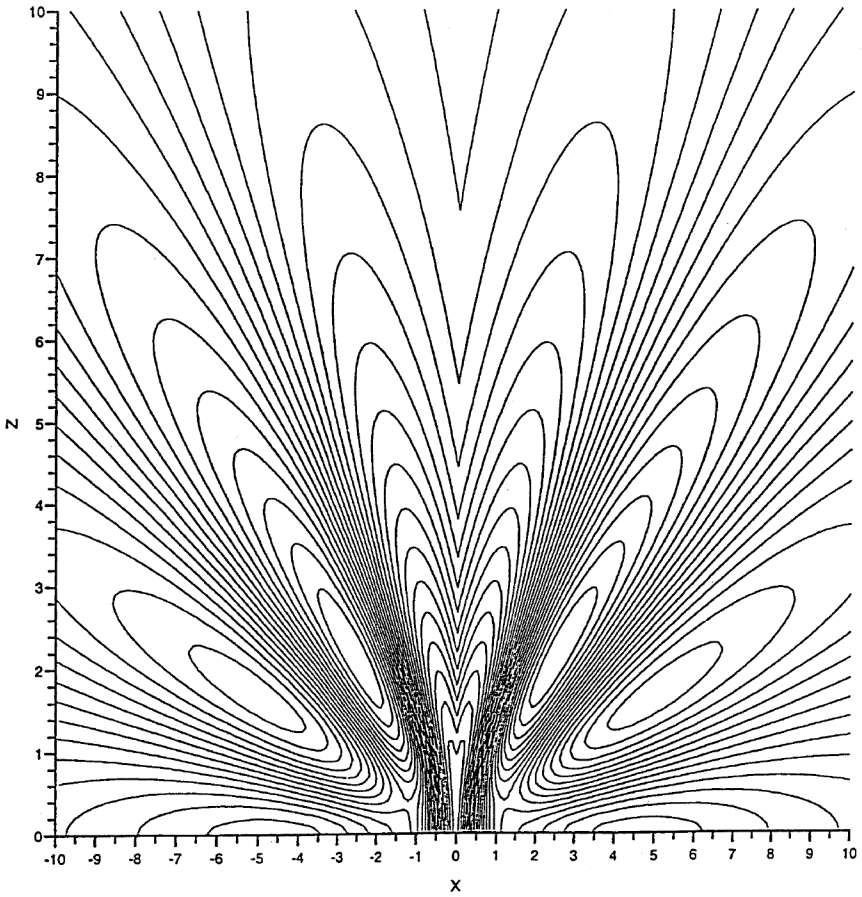

Figure 5. Spot produced in near-wake transition, given in planform at late time.

In the figure, on the left B is zero and an upstream convection and nonlinear bursting take place, whereas on the right B is large and suppresses bursting. Larger B values, corresponding to positions closer to the trailing edge, always produce amplitude decay.

Three-dimensional spots are also examined by Smith *et al.* An example indicating the late-time behaviour is presented in Figure 5.

4. Adverse pressure-gradient transition

The basic flow here is a boundary layer, on a smooth solid surface and subject to an 0(1) external pressure gradient $d\bar{p}/dx$. At the point of minimum pressure the velocity profile is $\bar{u}(\bar{y})$ say, with $\bar{u}''(0) = 0$ in view of the condition $\bar{p}'(0) = 0$. We also have $\bar{u}(0) = 0$, $\bar{u}'(0) = \bar{\lambda} > 0$ for attached forward motion, $\bar{u}'''(0) = 0$, while $\bar{u}'^{v}(0) = -24\kappa$ with κ positive. The above near-wall properties tie in with the profile $\bar{u}$ having negative curvature (no inflection) for all $0 < \bar{y} < \infty$, with $\bar{u}(\infty)$ being positive. However, inflection enters just downstream of the minimum pressure point since, at a typical such downstream station, $\bar{p}'$ is small, say $\bar{g}\sigma^2$, and so the basic profile near the wall is $\sigma\bar{\lambda}Y + \sigma^4(-\kappa Y^4 + \frac{1}{2}\tilde{g}Y^2)$ in effect. Again see Figure 1 *c*. Here $\bar{y}$ is σY with σ small, and $\tilde{g}$ is of order unity.

Hence for a three-dimensional disturbance it is found that

$$\omega_1 = \bar{u}^2(\infty)\alpha\gamma/\bar{\lambda}, \tag{9}$$

determines the leading order (real) part of the frequent response, essentially as anticipated in the introduction for area (iii). Here $\gamma^2 = \alpha^2 + \beta^2$ for spanwise wave number β. At a higher order the dominant growth rate

$$\omega_{4i} = \pi\tilde{g}\left(1 - \frac{\gamma^2}{\alpha_N^2}\right)\left(\frac{\bar{u}(\infty)}{\bar{\lambda}}\right)^4 |\alpha|\gamma^2 \tag{10}$$

is obtained, where $\alpha_N^2 \equiv \tilde{g}\bar{\lambda}^4/[12\kappa\bar{u}^4(\infty)]$.

With linear disturbances a three-dimensional spot forms, the evolution of the disturbance being given by a double Fourier (**) inversion,

$$4\pi^2\tilde{Q}(\tilde{x},\tilde{z},\tilde{t}) = \iint \tilde{Q}^{**}(k,\ell,0)\exp(K)\mathrm{d}k\mathrm{d}\ell, \qquad (11)$$

with, from (9), (10) with $\bar{u}(\infty), \bar{\lambda}$ unity,

$$K(k,\ell,\tilde{x},\tilde{z},\tilde{t}) \equiv \left[ik\hat{X} + i\ell\hat{Z} - ik(k^2+\ell^2)^{1/2} + \hat{g}\left\{1 - \frac{k^2+\ell^2}{\alpha_N^2}\right\} |k|(k^2+\ell^2)\right]\tilde{t}. \qquad (12)$$

Here the scaled spatial coordinates are $\tilde{x},\tilde{z}$, the scaled time $\tilde{t} \gg 1$ but $\hat{g}\tilde{t} \sim 1$, where $\hat{g} \equiv \sigma^3\pi\tilde{g}$ is small, while $(\hat{X},\hat{Z}) = (\tilde{x},\tilde{z})/\tilde{t}$ are 0(1) and k, ℓ are written for α, β respectively. The integral in eq. (11), with real k, ℓ, is taken over positive k because of symmetry. The initial condition $\tilde{Q}^{**}(k, \ell, 0)$ is $\exp(-q(k^2 + \ell^2)^{1/2})$ for example. To find the spot behaviour at large times a double steepest-descent method is used, giving the results in Figure 6.

Nonlinear effects lead on to structural change of the above fluctuating disturbances, occurring first at the spot leading edge. There is also an alteration of the mean flow. The result of most immediate interest there is

$$\partial_T(u_m) = -\frac{1}{2}a_0 a_{0X}, \qquad (13)$$

giving the induced mean wall slip under and ahead of the spot, subject to the initial condition $u_m = 0$ at time $T = 0+$ for all positive X. Here a_0 is the scaled fluctuating disturbance amplitude. This confirms that at a given streamwise position the main fluctuations sweep by, leaving mean-flow alterations behind. The solution is presented in Figure 7 for different initial fluctuation amplitudes. At comparatively low input amplitudes this mean-flow solution continues for a long way downstream, and for a relatively long time, developing an exponentially growing and expanding form in η, T at large T. Here η is X/T. We observe also the similarity form holding at the start, for small T, in which Tu_m is a function of η, along with $T^{1/2}a_0$, this form being accommodated in the computations. At medium input amplitudes the nonlinear solution clearly terminates at a finite time, as indicated by a_0 attaining its maximum value. This termination time becomes shorter with increasing input. Also, in most cases there is a pronounced expanding region where the induced mean velocity u_m is negative, this region moving with the spot and supplementing the fixed region of positive and negative velocity values which trails behind. The above is for X and T positive, whereas the mean vorticity alteration, like u_m, is zero for X negative behind the spot trailing edge, where another mechanism acts.

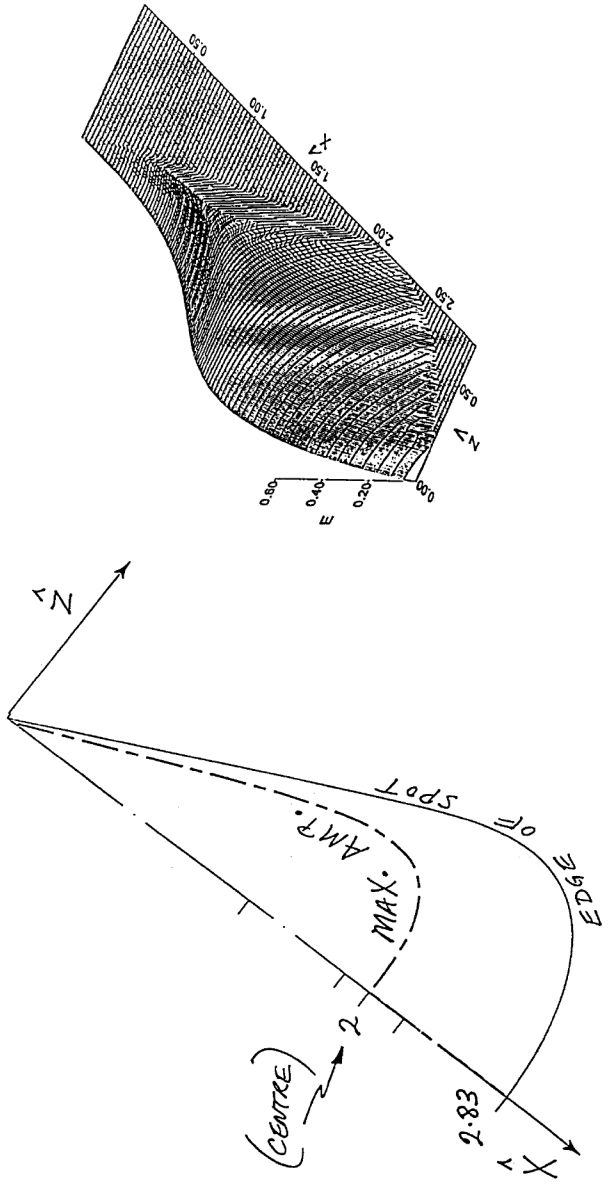

Figure 6. Large-time spot in the adverse pressure gradient case, showing planform and representative amplitude E vs $\hat{X},\hat{Z}$.

5. Further comments

We end with some brief comments. Regarding area (i) (roughnesses), the transition onsets studied here are not associated with the first appearance of an adverse pressure gradient as there is a delay such that the critical inflection point occurs mid-flow in the sublayer. The flow conditions there govern whether the motion locally is subcritical or supercritical and in addition they determine the crucial coefficients $\bar{A} - \bar{D}$ via integral properties, once (1) is satisfied. The disturbance behaviours noted in §2 lead on to new flow structures at increased times, as transition to turbulence continues beyond the present scope.

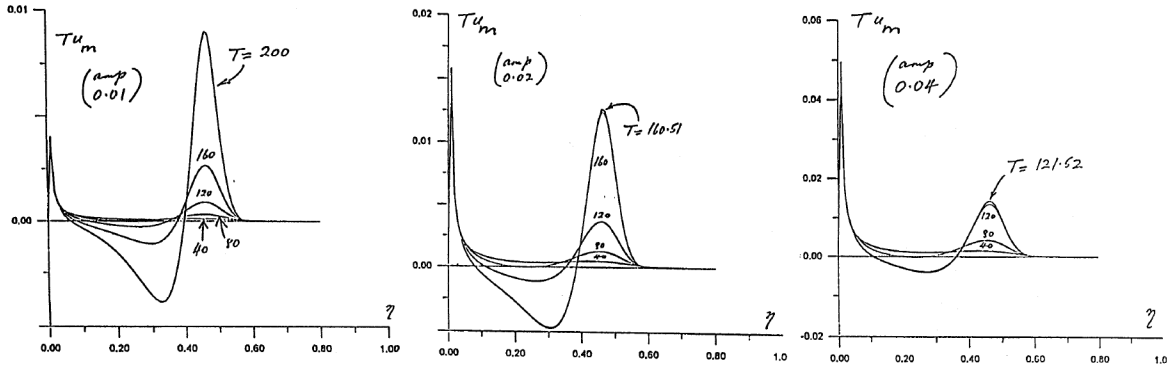

Figure 7. Nonlinear temporal development of the mean flow alteration u_m vs η for three amplitudes of initial disturbance, increasing from the left. Leading edge break-up occurs at the final times marked in the middle and right-hand graphs.

A further motivation for the study in (i), apart from the context of surface imperfections, is related to the effects of an adverse pressure gradient on spots in boundary layers. The substantial observed enhancement of the spanwise spreading rate of the spot, under an adverse pressure gradient, is an especially noteworthy feature compared with the case of a zero or favourable pressure gradient. The trend seen in the present results is one of relatively increasing spanwise spreading of the spot as the adverse parameter G in Figure 2 increases. Tentatively therefore, the present theoretical findings bear some resemblance, albeit loose as yet, to the above experiments, granted that the experimentally observed spots are turbulent whereas the theory assumes laminar motion and that the spatial scales and characteristic speeds of the theoretical spot are smaller.

Another application concerning the theory in (i) is in the onset of relatively high-frequency three-dimensional disturbance components at the first-spike stage in deep transition. Transitional disturbances leading to spots in a laminar boundary layer were investigated by Breuer *et al.*, experimentally, following studies by Henningson *et al.*, Kachanov and Shaikh and Gaster, while related theoretical work is by Hoyle *et al.*, Smith and Bowles, and others, partly connected with the condition (1). In this application also, disturbances of predominantly inviscid form with high typical frequencies and comparatively small amplitudes initially come into play because of the local positive growth rates that are induced. These are described as in §2.

Regarding area (ii) (near wakes), destabilization further to that described in §3 can be induced by nonsymmetric velocity profiles and by even a small amount of reversed flow. We add that the arguments involved in area (ii) should extend to separating flows also.

Regarding area (iii) (adverse pressure gradients), Smith and Timoshin also consider the approach to separation and different types of disturbance initiation, including wall forcing and vortical wake passing.

Links with experiments are considered in the three original papers, as are certain further studies. There have been a few quantitative comparisons with experiments or simulations, for example with Nishioka *et al.*, on the criterion (1) in area (i) and with Hannemann and Oertel on the predictions in area (ii) but more are desirable. Recent numerical simulations concerning area (ii) have been performed by C. Davies and show agreement with (7) so far.

1. Savin, D. J., Smith, F. T. and Allen, T., *Proc. R. Soc.*, 1999, **A455**, 491–541.
2. Smith, F. T., Bowles, R. G. A. and Li, L., *Eur. J. Mech.*, 2000, **19**, 173–211.
3. Smith, F. T. and Timoshin, S. N., *J. Fluid Mech.*, 2000, to appear.
4. Narasimha, R., Report of workshop on boundary layer transition in turbomechanics, Minnowbrook II, Syracuse, New York, Sept. 1997, NASA/CP-1998-206958.
5. Brown, S. N. and Smith, F. T., *Q. J. Mech. Appl. Math.*, 1999, **52**, 269–281.